Dalton Transactions

The fascinating story of axial ligand dependent spectroscopy and redox-properties in iron(II) phthalocyanines

Journal:	*Dalton Transactions*
Manuscript ID	DT-FRO-08-2023-002565.R1
Article Type:	Frontier
Date Submitted by the Author:	06-Sep-2023
Complete List of Authors:	Ziegler, Christopher; University of Akron, Department of Chemistry Nemykin, Viktor; The University of Tennessee Knoxville, Department of Chemistry

The fascinating story of axial ligand dependent spectroscopy and redox-properties in iron(II) phthalocyanines

Christopher J. Ziegler† and Victor N. Nemykin‡

† *Department of Chemistry, University of Akron, Akron, OH 44325, United States*

‡ *Department of Chemistry, University of Tennessee, Knoxville, TN 37996, United States*

Abstract: Iron phthalocyanines play crucial fundamental and applied roles ranging from bulk colorants to components of advanced materials. In this mini-review, we discuss four aspects concerning the influence of the axial ligands on spectroscopic and redox properties of iron(II) phthalocyanines: (i) iron versus macrocycle oxidation cite as a function of Lever's E_L parameter; (ii) energy of the metal-to-ligand charge-transfer transitions as a function of Lever's E_L parameter; (iii) iron versus macrocycle reduction in iron(II) phthalocyanines; (iv) Mössbauer quadrupole splitting as a function of axial ligand binding through the prism of d_{z2} orbital population.

Introduction

For inorganic chemists, phthalocyanine (Pc(2-)) remains one of the most important ligand systems, exhibiting chemistry that spans across the periodic table.[1,2] Indeed, more than 34,000 research papers and 19,000 patents have been published on phthalocyanine systems (based on Web of Knowledge database accessed on August 1, 2023). Since its appearance in the early years of the 20th century, phthalocyanine has held important roles as bulk colorants as well as components of advanced materials. As dyes, phthalocyanines and its metal adducts represent a 2.5-billion-dollar

market, with an annual production of more than 80,000 metric tons.[1] Both the free base and its metal adducts have been studied for their fundamental properties, and in addition to their uses as colorants, have found applications in (opto)electronic devices, sensors, and catalysts.[3-5] The majority of its applications are based on the bright optical properties of the phthalocyanine chromophore (Figure 1) that are reflective of the π–π* transitions in the aromatic macrocycle. The optical properties of the phthalocyanines can be modified via peripheral substitution.[6] However, the introduction of a transition-metal with a partially filled d-subshell (typically d^3-d^7 electronic configurations) offers the additional opportunities for observation of charge-transfer (CT) transitions in these systems. The energies of such bands depend on the electronic structure of the phthalocyanine core, nature of the central ion, and the electronic properties of the axial ligands. Iron is particularly notable in this regard, as not only does the oxidation state of the metal alter the potential energies of the d-orbitals, but the identity of the axial ligands also can affect the optical transitions and the other spectroscopic properties seen in iron phthalocyanines. In this paper, we summarize some of our recent results on the systematic tuning of the energies of iron d-orbitals by the axial ligation in low-spin iron(II) phthalocyanines (Pc(2-)Fe^{II}) on selected properties of these systems.

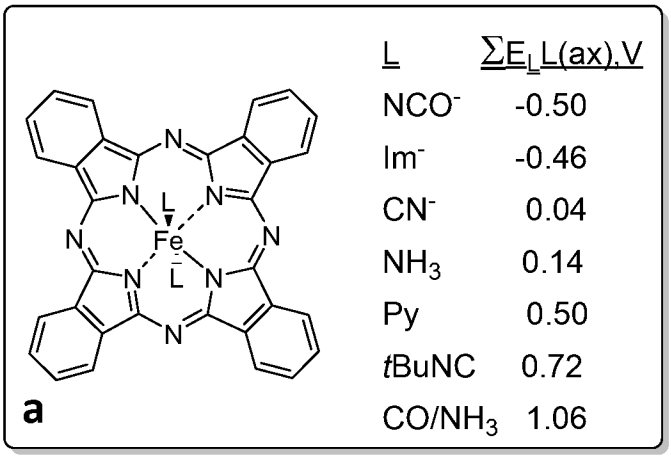

Figure 1. Representative examples of axially coordinated iron(II) phthalocyanines (a); X-ray crystal structure of $Pc(2-)Fe^{II}(DABCO)_2$ (b).

How the electronic and steric properties of the axial ligands manipulates the site of oxidation in iron(II) phthalocyanine systems.

In 1990, Lever introduced an electrochemically based redox parameter $E_L(L)$ to quantify the effects of ligands on Ru(II)/Ru(III) oxidation potentials.[7] Like the Hammett parameter, the $E_L(L)$ parameter accounts for both σ and π contributions of axial ligand as well as steric bulk. The original Equation to predict half wave potentials is shown in Eq. 1, where S_M and I_M are metal- and spin-state dependent scaling and offset factors, respectively.

$$E_{\frac{1}{2}}(Ru(II)/Ru(III)) = S_M\sum E_L(L) + I_M \quad (1)$$

For phthalocyanines, the equatorial positions are occupied by the macrocycle, and if the same phthalocyanine is used, the effect of ligand's variation is thus limited to the axial position. This results in Eq. 2, and Lever demonstrated that for a limited series of Fe(II) and Fe(III) phthalocyanines, half wave potentials could be successfully predicted using the axial $E_L(L_{ax})$ parameter alone.[8]

$$E_{\frac{1}{2}}(Fe(II)/Fe(III)) = S_M\sum E_L(L_{ax}) + I_M \quad (2)$$

Equation (2) allows a potential crossover between the phthalocyanine-centered HOMO of a_{1u} symmetry (in a standard Gouterman's D_{4h} point group notation)[9] and iron-centered d-orbitals (Figure 2).[10] Indeed, one might assume that axial ligands with strong π-acceptor properties would stabilize the iron-centered d_π orbitals below the energy of a_{1u}. In this case, phthalocyanine-based oxidation is expected.

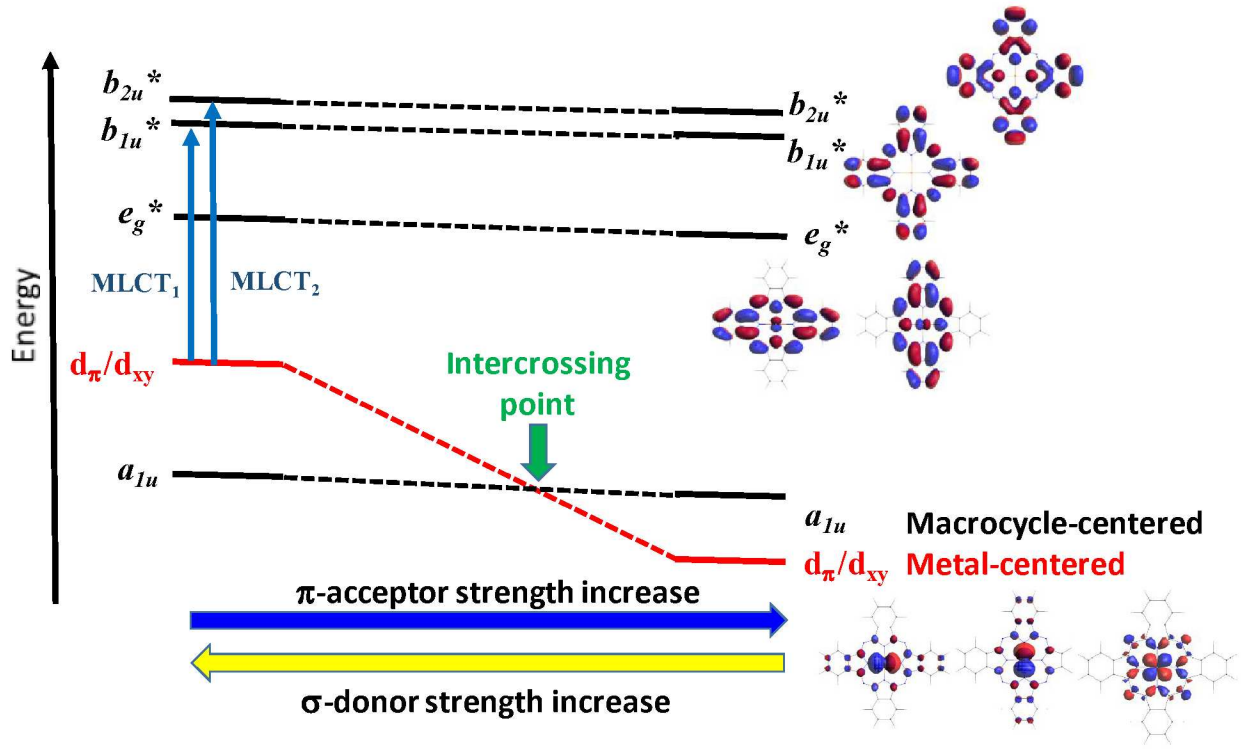

Figure 2. Simplified energy diagram of selected frontier orbitals of Pc(2-)Fe^{II}L$_2$ complexes.[10] Adapted with permission from *Inorg. Chem.* **2021**, *60*, 16626-16644. Copyright 2021 American Chemical Society.

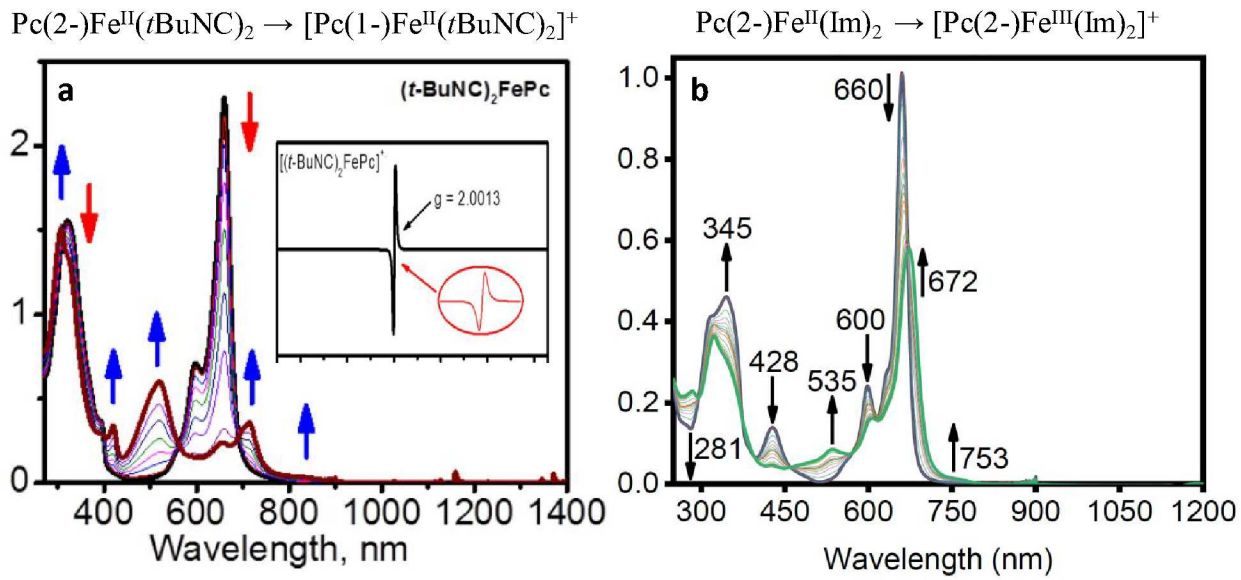

Figure 3. Oxidation of Pc(2-)$Fe^{II}L_2$ complexes to $[Pc(1-)Fe^{II}L_2]^+$ (a)[11] and $[Pc(2-)Fe^{III}L_2]^+$ (b)[10] species under spectroelectrochemical conditions.

Indeed, a decade ago, we observed the formation of the phthalocyanine cation-radical during oxidation of Pc(2-)Fe^{II}(*t*BuNC)$_2$ complex (Figure 3).[11] More recently,[10] we conducted a systematic analysis of the Pc(2-)$Fe^{II}L_2$, Pc(2-)$Fe^{II}L'L''$ and $[Pc(2-)Fe^{II}X_2]^{2-}$ complexes using electro- and spectroelectrochemical methods coupled with DFT calculations to identify the crossing point shown in Figure 2. Figure 1 shows the structures of several such complexes, which includes both anionic and neutral ligands as well as a variety of donor atom types including carbon, nitrogen, phosphorous, and sulfur. The Lever's electrochemical parameters are shown next to the structures in the Figure. The more negative values of E_L, the greater the destabilization of the d_π orbitals on the iron center. With more positive E_L values, the iron-centered orbitals become lower in energy. To determine the identity of the HOMO orbital in these iron phthalocyanine systems with axial ligands, we employed spectroelectrochemical or chemical oxidation experiments.[10] Upon oxidation, it is relatively straightforward to determine if the oxidation event is metal or macrocycle localized. For metal centered oxidations, we observe a low energy shift and reduction in intensity of the Q-band along with the raise of CT band in ~540-570 nm area, corresponding to a low spin (S = ½) Fe(III) system. A good example of this is observed in the Pc(2-)Fe^{II}(Im)$_2$ spectroelectrochemical oxidation, as shown in Figure 3. This process is fully reversible and is indicative of a metal centered electron abstraction process. The crossover to ring based oxidation only takes place at the very strong field limit. In contrast, as seen in the spectra of Pc(2-)Fe^{II}(RNC)$_2$ compounds, removal of an electron from the π system results in significantly different effects in its UV-Vis spectrum. Upon oxidation, the Q-band disappears and a series of three bands at ~700,

~525, and ~420 nm appears, which are characteristic for the formation of the ring-based radical cation. EPR experiments of this complex reveal a g-value around that of the free electron, as would be expected for a π-based radical system.[11] If the contribution from the phthalocyanine ring is constant, then there should be a direct relationship between the observed Fe(II)/Fe(III) electrochemical potential and the Lever parameter E_L (eq. 2). When the first oxidations of Pc(2-)$Fe^{II}L_2$, Pc(2-)$Fe^{II}L'L''$, and $[Pc(2-)Fe^{II}X_2]^{2-}$ are graphed versus this parameter, a two-slope correlation is revealed, similar to that seen in a Job plot, shown in Figure 4.

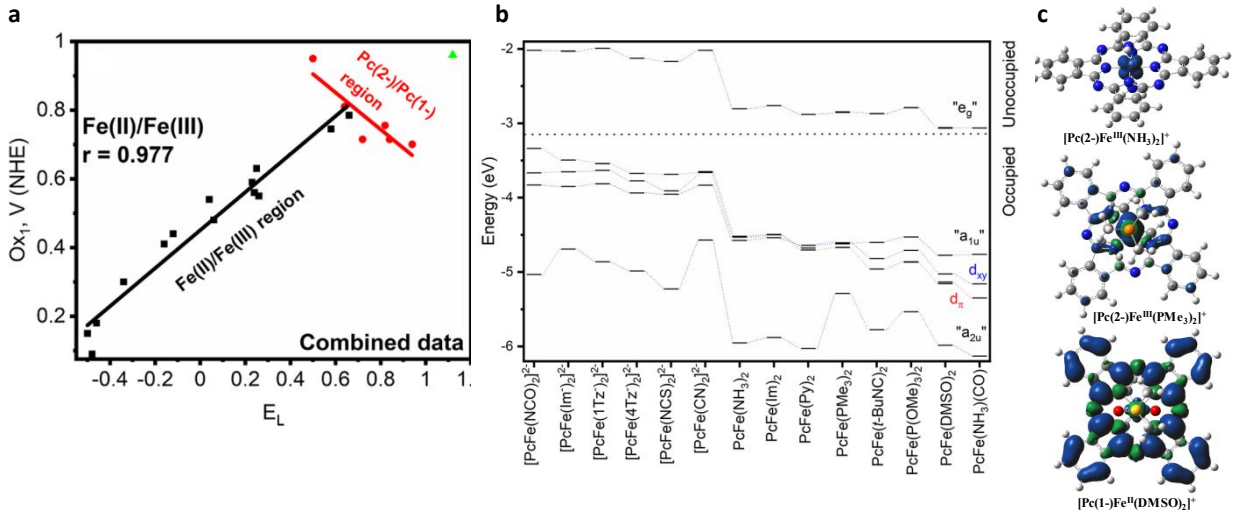

Figure 4. Correlations between oxidation potentials and $\Sigma E_L L(ax)$ (a), DFT-predicted energy diagram for Pc(2-)$Fe^{II}L_2$ complexes (b); DFT-predicted spin densities in selected $[PcFeL_2]^+$ complexes (c).[10] Adapted with permission from *Inorg. Chem.* **2021**, *60*, 16626-16644. Copyright 2021 American Chemical Society.

The presence of the second slope is in good agreement with the electronic model where the increasing stabilization of the metal d_{xy} and d_π orbitals causes them to intersect with the phthalocyanine π-orbitals, specifically the Gouterman-type a_{1u} orbital.[10] Beyond this intersection point, the HOMO becomes phthalocyanine π-orbital in character, and oxidation results in π radical-

cation rather than low spin Fe(III) ion formation. For the iron-based oxidation region for all PcFe complexes studied (with the exception of the Pc(2-)Fe^{II}(n-$BuNH_2$)(CO) complex), the correlation coefficient between oxidation potentials and the E_L parameter is 0.997 in polar solvents. For the Pc(2-)Fe^{II}(n-$BuNH_2$)(CO) compound, the iron ion resides significantly outside the plane of the phthalocyanine porphyrin, resulting in a deviation in oxidation potential. Using the combined data, we recalculated the correlation as $E_{½}$ (Fe(II)/Fe(III), NHE) = 0.55 $\Sigma E_L(L_{ax})$ + 0.45 which is similar to that reported by Lever on a smaller number of compounds ($E_{½}$ (Fe(II)/Fe(III), NHE) = 0.76 $\Sigma E_L(L_{ax})$ + 0.52). The DFT calculations agree well with the theoretical predictions and experimental data. All three tested exchange-correlation functionals (MPWLYP, TPSSh, and O3LYP) predict crossover of the iron d-orbitals with the Gouterman-like a_{1u} orbital of the phthalocyanine ring. The exact point of crossover depends on the exchange-correlation used in the calculation (Figure 4). Both, experimental observations and DFT calculations suggest the crossing point around $\Sigma E_L L(ax)$ = 0.5 -0.6 V, which is close to the value for two axial pyridine ligands. This allows us to raise an interesting question on the fine tuning of the electronic structure of the axial substituted pyridine ligands in Pc(2-)$Fe^{II}L_2$ complexes that would lead to the energetically equivalent iron-centered d_π and phthalocyanine-centered a_{1u} orbitals. In this case, thermally activated electron-migration driven valence tautomerism between transition metal and macrocycle is possible, i.e.: $[Pc(1-)Fe^{II}L_2]^+ \leftrightarrow [Pc(2-)Fe^{III}L_2]^+$. These systems might have a set of rather unique spectroscopic and magnetic properties.

How the electronic and steric properties of the axial ligands affects the energies of MLCT transitions in iron(II) phthalocyanine systems.

In 1968,[12] Dale reported that in Pc(2-)$Fe^{II}L_2$ and $[Pc(2-)Fe^{II}X_2]^{2-}$ compounds, the absorption bands between 420 and 455 nm were highly contingent on axial ligand identity. This dependency was attributed to a metal-to-ligand CT (MLCT) character in these bands. Later work by Stillman and coworkers investigated small set of Pc(2-)$Fe^{II}L'L''$ and $[Pc(2-)Fe^{II}X_2]^{2-}$ complexes with UV-visible and magnetic circular dichroism (MCD) techniques, and further deconvoluted their absorption spectra.[13] Stillman hypothesized that the lowest energy axial ligand dependent transition, which manifests as a MCD Faraday A-term observed in the 455−360 nm region, primarily results from an e_g (Fe, d_π) → b_{1u}* (Pc, π*) single-electron process (Figure 5). As a result, the energy of this band mostly reflects the relative energy level of the iron centered d_π orbitals. An earlier attempt to rationalize the energy of the MLCT band as a function of σ-donor, π-acceptor, and steric properties of the axial ligands was made by us more than two decades ago.[14] Additionally, Sumimoto and coworkers used computations to elucidate the electronic structures of Pc(2-)Fe^{II}(Py), Pc(2-)$Fe^{II}(Py)_2$, Pc(2-)Fe^{II}(CN−) and Pc(2-)$Fe^{II}(CN-)_2$ complexes with limited success.[15]

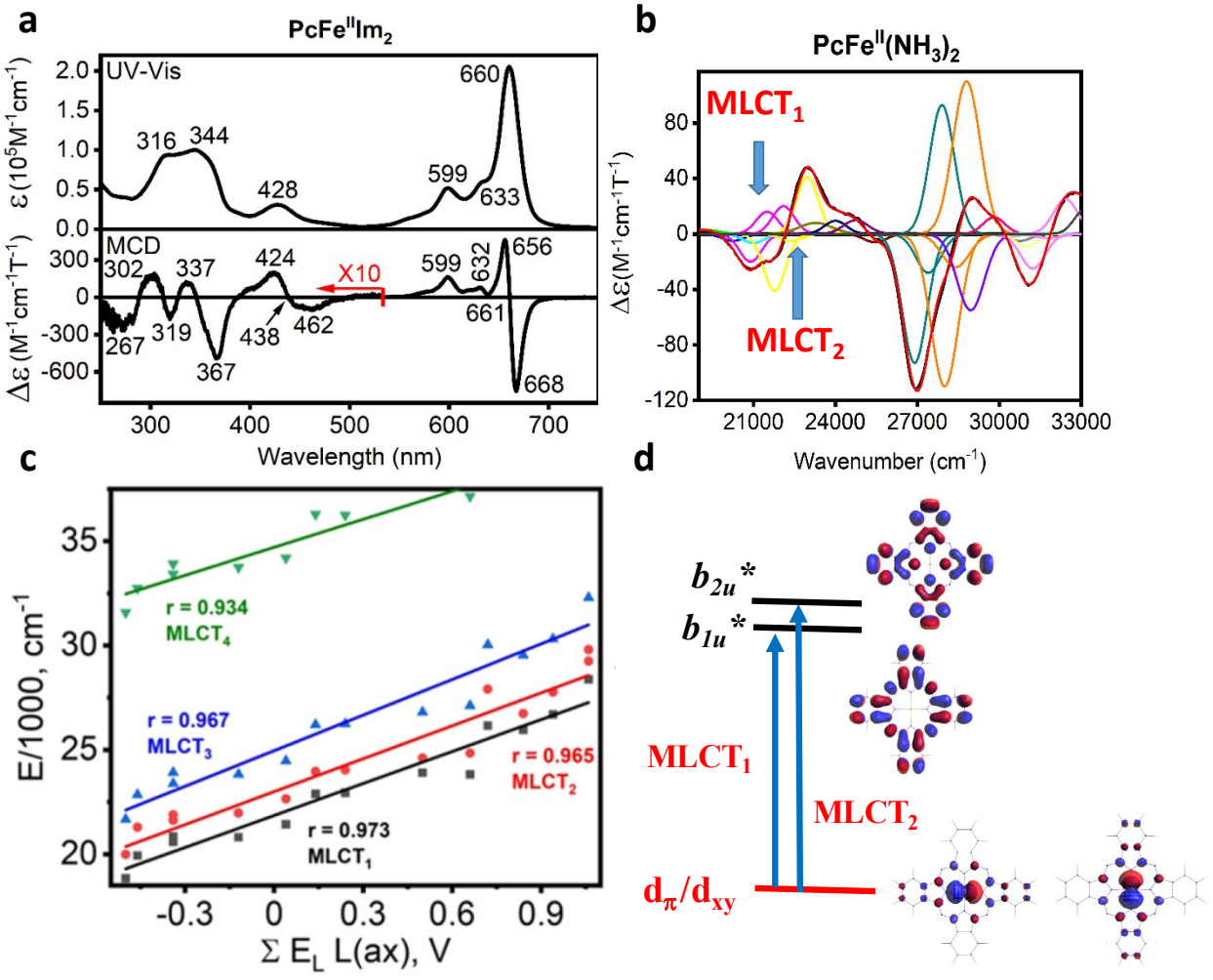

Figure 5. Representative example of UV-Vis and MCD spectra of Pc(2-)Fe^{II}L$_2$ complexes (a); deconvolution analysis of the MLCT1 and MLCT2 bands in Pc(2-)Fe^{II}(NH$_3$)$_2$ (b); correlations MLCT$_{1\text{-}4}$ bands and $\Sigma E_L L(ax)$ (c); simplified representation of MLCT$_1$ and MLCT$_2$ transitions (d).[16] Adapted with permission from *Inorg. Chem.* **2022**, *61*, 8250-8266. Copyright 2022 American Chemical Society.

In a new attempt to investigate this phenomenon,[16] we hypothesized that there should also be a correlation between the Lever electrochemical parameter E_L and the energy of the first (lowest energy) MCD A term between 500 and 350 nm. Indeed, if the relative energies of the

phthalocyanine-centres MOs are nearly constants, then the d_π(Fe)- b_{1u}* (Pc,π*) gap should be solely a function of the sum of E_L parameters of the axial ligands (eq. 2 and Figure 5d). Thus, Lever's E_L scale[7] can also be used for the prediction of the energy of MLCT transitions in Pc(2-)$Fe^{II}L_2$, Pc(2-)$Fe^{II}L'L''$, and $[Pc(2\text{-})Fe^{II}X_2]^{2-}$ complexes. The theoretical relationship between this $e_g \rightarrow b_{1u}$* transition and the frontier orbitals, which is metal to ligand charge transfer in character for those systems where the HOMO is d-orbital in character, can be described by the following Equation (eq. 3):[15]

$$E_{MLCT} = F\sum E_L L(ax) + const \qquad (3)$$

This expression is very similar to the expression shown in Equation 2, and one would expect that there would be a direct dependence on the axial Lever's electrochemical parameter and the energy of the MLCT transition (eq. 3). To observe if there is a correlation between the lowest energy MLCT band and the Lever electrochemical parameter, we collected the MCD spectra of a series of Pc(2-)$Fe^{II}L_2$, Pc(2-)$Fe^{II}L'L''$, and $[Pc(2\text{-})Fe^{II}X_2]^{2-}$ complexes. The spectra show similar features with the MLCT bands clearly appear in the 400-500 nm region. UV-Vis and MCD spectra deconvolution analysis of a series of Pc(2-)$Fe^{II}L_2$, Pc(2-)$Fe^{II}L'L''$, and $[Pc(2\text{-})Fe^{II}X_2]^{2-}$ complexes coupled with TDDFT calculations allowed us to identify two closely spaced (0.1-0.2 eV) pairs of degenerate, xy-polarized $MLCT_{1\text{-}2}$ transitions arise from e_g (Fe, d_π) → b_{1u}*, b_{2u}* in the visible region (Figure 5). Prior observations by Stillman and Sumimoto agree with our overall calculations.[13,15]

As expected from Equation 3, the experimental and TDDFT-predicted energies of the $MLCT_1$ and $MLCT_2$ correlate well with the Lever electrochemical parameter E_L (Figure 5).[16] The energies of the bands that are of π–π* character do not show any dependence on E_L values. For the experimental data, the slopes of the MLCT lines are nearly identical. Based on the data from

the deconvoluted MCD spectra, we were able to express Equations to predict $MLCT_2$ bands in $Pc(2\text{-})Fe^{II}L_2$, $Pc(2\text{-})Fe^{II}L'L''$, and $[Pc(2\text{-})Fe^{II}X_2]^{2-}$ complexes in both UV-visible spectra (Equation 4) and the A-term in MCD spectra (Equation 5).

$$E_{MLCT}(UV-vis, cm^{-1}) = 2720\sum E_L L(ax) + 23174 \quad (4)$$

$$E_{MLCT}(MCD, cm^{-1}) = 2444\sum E_L L(ax) + 22402 \quad (5)$$

Equations 4 and 5 enable fast estimation of the MLCT transition energies in the low-spin iron(II) phthalocyanines as well as set the limits for the energies of such transitions.

How reduction occurs in axially coordinated iron(II) phthalocyanines.

The energy gap between phthalocyanine-centered b_{1u}* and b_{2u}* orbitals (Figure 2) that gives a raise to $MLCT_1$ and $MLCT_2$ transitions in $Pc(2\text{-})Fe^{II}L_2$, $Pc(2\text{-})Fe^{II}L'L''$, and $[Pc(2\text{-})Fe^{II}X_2]^{2-}$ complexes can be estimated from the UV-Vis and MCD data of $[Pc(3\text{-})Fe^{II}L_2]^{-}$, $[Pc(3\text{-})Fe^{II}L'L'']^{-}$. and $[Pc(3\text{-})Fe^{II}X_2]^{3-}$ complexes as shown in Figure 6. Thus, we decided to probe the reduction chemistry of iron phthalocyanines.[17] The single electron reduction of $PcFe^{II}$ compounds has not been well explored. We would expect, however, to observe similarly complex ligand-dependent behavior in the single electron reduction of $Pc(2\text{-})Fe^{II}L_2$, $Pc(2\text{-})Fe^{II}L'L''$, and $[Pc(2\text{-})Fe^{II}X_2]^{2-}$ complexes. There has been some prior work on the reduction of $Pc(2\text{-})Fe^{II}$ compounds starting in the 1960s and 1970s. In 1972, Clack and Yandle reported the UV−vis spectrum of sodium metal reduced iron phthalocyanine,[18] and in 1974 Taube presented the first Mössbauer spectrum of a reduced $Pc(2\text{-})Fe^{II}$ compound.[19] in 1978, Lever and Wilshire reported a UV−vis spectrum and a solution EPR spectrum of a single-electron-reduced iron phthalocyanine, which seemed to indicate that the metal, rather than the phthalocyanine ring, is the site of reduction.[20] The EPR spectra in various solvents with coordinating axial ligands (DMSO, DMA, Ph_3P,

imidazole, and pyridine) revealed axial spectra with $g_{\perp}$ between 2.077 and 2.119 and $g_{||}$ between 1.953 and 1.961 were indicative of a Fe(I) (d^7) system. The superhyperfine coupling was also indicative of a metal-based reduction process and a loss of one of the axial ligands. At the same time, the UV-visible spectrum of the reduction product was more indicative of a phthalocyanine ring-based radical-anion rather than a metal-centered reduction. Although Kobayashi[21] and Konarev[22] separately noted the radical nature of the UV-visible spectra in single electron reduced Pc(2-)Fe^{II} compounds, Lever's initial interpretation was undisputed. Regardless, structural elucidation and magnetometry studies of reduced Pc(2-)Fe^{II} compounds are consistent with the electron stoichiometry as well as their S = ½ ground state character.

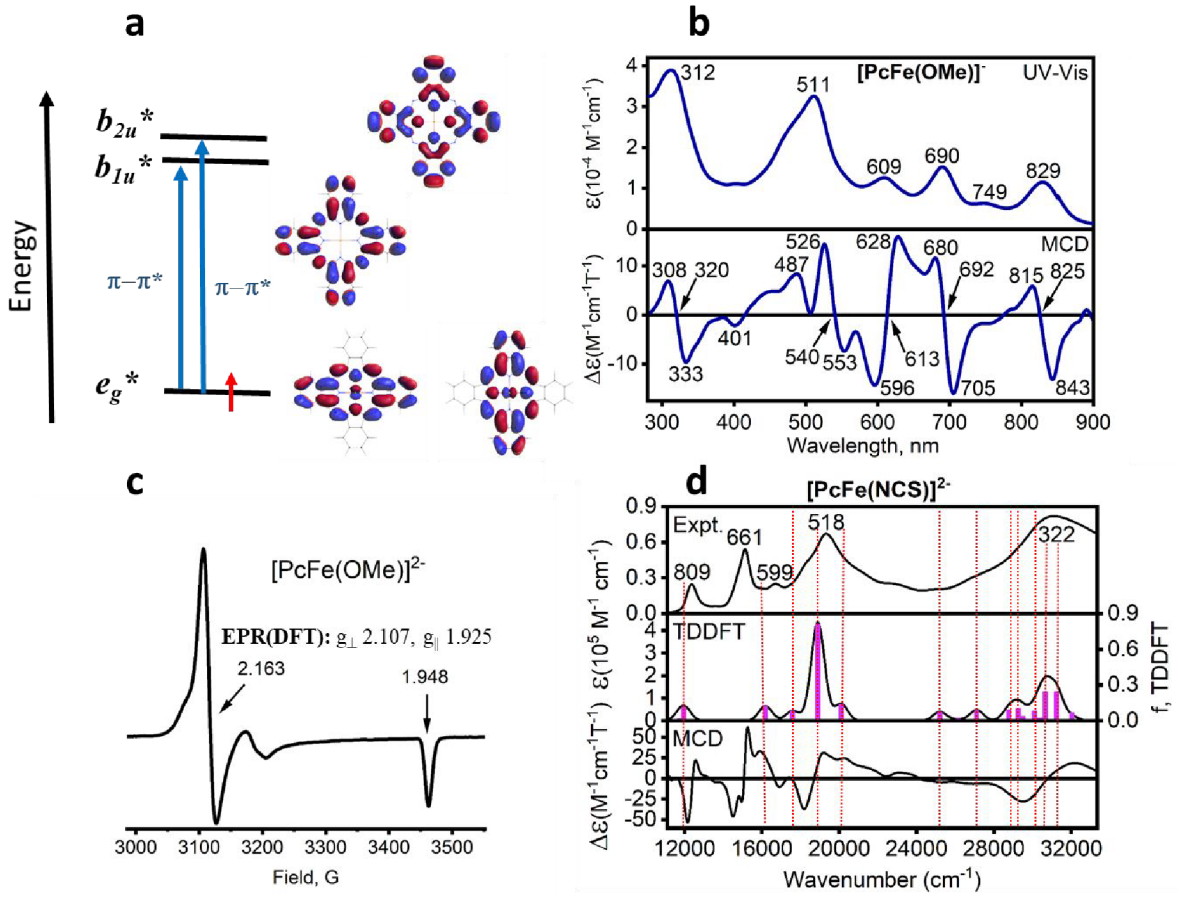

Figure 6. Simplified energy diagram for $[Pc(3-)M^{II}]^-$ complex showing two π–π* transitions that allow direct measure of b_{1u}*-b_{2u}* energy gap (a); representative example of UV-Vis and MCD spectra of $[PcFeL]^-$ complexes (b); representative example of EPR spectra of $[PcFeL]^-$ complexes (c).[17] comparison between the experimental and TDDFT-predicted UV-Vis and MCD spectra of $[PcFe(NCS)]^{2-}$ complex; vertical dashed lines show the TDDFT-predicted degenerate transitions (d). Adapted with permission from *Inorg. Chem.* **2022**, *61*, 20177-20199. Copyright 2022 American Chemical Society.

To re-examine this fundamental question of the metal or ring-based reduction in $Pc(2-)Fe^{II}L_2$, $Pc(2-)Fe^{II}L'L''$, and $[Pc(2-)Fe^{II}X_2]^{2-}$ complexes we looked at structural, spectroscopic, and theoretical data for evidence of a $[Pc(2-)Fe^{I}L]^-$ versus a $[Pc(3-)Fe^{II}L]^-$ assignment.[17] Investigations into the electrochemistry and spectroscopy of the reduction of $Pc(2-)Fe^{II}L_2$ and $[Pc(2-)Fe^{II}X_2]^{2-}$ can be highly complex, as the reduction can change the affinities for axial ligands. Notably, we observed the formation of five coordinate rather than six coordinate species upon reduction. For example, reduction of the $Pc(2-)Fe^{II}(DMSO)_2$ complex can result in loss of one of the axial ligands and possible replacement by the other ligand such as PPh_3. In general, chemical and spectroelectrochemical reduction of $Pc(2-)Fe^{II}L_2$ and $[Pc(2-)Fe^{II}X_2]^{2-}$ results in similar spectroscopic changes. Reduction results in loss of the Q band between 650 and 655 nm as well as the $MLCT_{1-2}$ transitions between 410 and 460 nm. Additionally, new bands appear at ~800, ~690, ~600 and ~515 nm (Figure 6). We used MCD to investigate the spectra of these reduced PcFe compounds, and once again the reduction spectra are very similar with some small dependence on the identity of the axial ligand.[17] The UV-visible and MCD spectra resemble those of $[Pc(3-)M^{II}]^-$ complexes such as those seen for the closed-shell metals $Mg^{2+}$and Zn^{2+} and are

indicative of a single electron reduction of the phthalocyanine ring, and so we can characterize these derivatives as $[Pc(3\text{-})Fe^{II}]^{-}$, $[Pc(3\text{-})Fe^{II}L]^{-}$, or $[Pc(3\text{-})Fe^{II}X]^{2-}$ species. This electronic ring-based reduction assignments, however, seemingly contradicts the solution EPR data collected by Lever and Wilshire in 1978[20] as well as later work by Dzilinski in 2007.[23] Indeed, we collected EPR spectra (Figure 6) of frozen solutions of $[PcFeL]^{-}$ and $[PcFeX]^{2-}$complexes and the resultant spectra are exhibit features consistent with a S = ½ d^7 metal center. We observe axial EPR spectra with clear hyperfine coupling with axial ligands such as PPh_3. Other spectroscopic observations provide mixed evidence for ring or metal-based reduction. The paramagnetic character of these compounds was confirmed by ^1H NMR spectroscopy along with Evan's method magnetic susceptibility measurements. The Mössbauer spectra of the reduced complexes reveal larger quadrupolar splittings than seen in the $Pc(2\text{-})Fe^{II}$ compounds which is at first glance more consistent with a Fe(I) assignment, but we later determined that increasing electron density at the metal center (vide infra) could also explain these splitting without reducing the metal.[17]

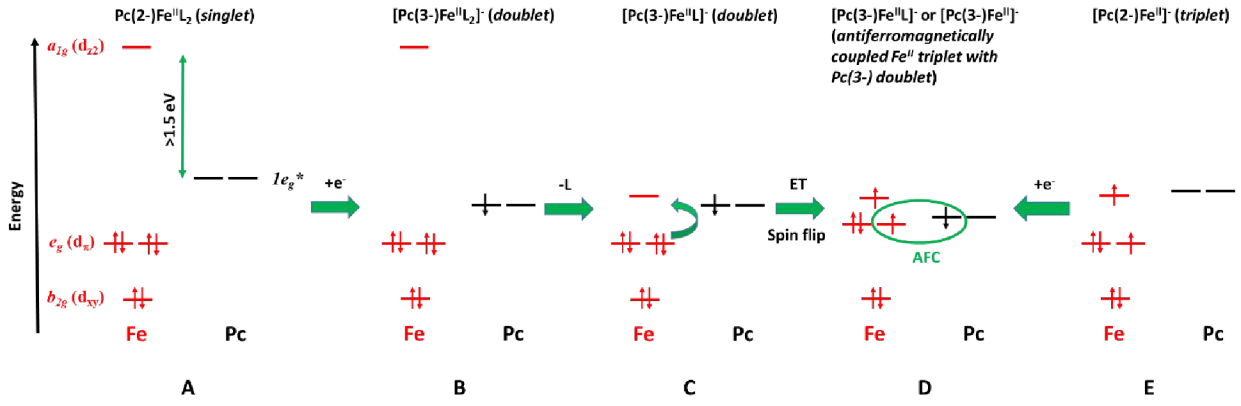

Figure 7. Proposed mechanism of the formation of the $[Pc(3\text{-})Fe^{II}]^{-}$ and $[Pc(3\text{-})Fe^{II}L]^{-}$ complexes from $Pc(2\text{-})Fe^{II}L_2$ and $Pc(2\text{-})Fe^{II}$ compounds upon single-electron reduction.[17] Adapted

with permission from *Inorg. Chem.* **2022**, *61*, 20177-20199. Copyright 2022 American Chemical Society.

The contradictory spectroscopic observations on iron phthalocyanine reduction can be resolved by using DFT and TDDFT calculations, which are indicative of the following steps during reduction process (Figure 7): (i) initial reduction of the phthalocyanine core; (ii) dissociation of one of the axial ligands and stabilization of the iron-centered d_{z2} orbital; (iii) transformation of the iron(II) center from low-spin to intermediate-spin (s=1); (iv) antiferromagnetic coupling between $(d_\pi)^3$ and $(e_g^*)^1$ orbitals. This explains the overall susceptibility and in the TDDFT predicted spectra, can predict the radical anion character in the phthalocyanine ring. Calculated EPR, Mössbauer, and UV-Vis spectra of $[Pc(3-)Fe^{II}L]^-$ and $[Pc(2-)Fe^{II}X]^{2-}$complexes are in excellent agreement with the experimental data. As predicted by TDDFT calculations for $Pc(2-)Fe^{II}L_2$ complexes, MCD spectra of $[Pc(3-)Fe^{II}L]^-$ and $[Pc(3-)Fe^{II}X]^{2-}$complexes show small b_{1u}^*-b_{2u}^* energy gap.

How iron(II) phthalocyanines exhibit a large span of Mössbauer quadrupole splittings

One of the fascinating aspects of the low-spin axially coordinated iron(II) phthalocyanines is their large span of the Mössbauer quadrupole splittings, which can range between ~0.7 and ~2.9 mm/s.[16,24-28] The higher values are even larger than those found in the intermediate-spin (s=1) $Pc(2-)Fe^{II}$.[27] In simplified point-charge model, Mössbauer quadrupole splitting can be estimated from the sum of the valence and lattice contributions shown in Equations 6 and 7.

$q_{val} = (4/7)\,(1-R)\,\langle r^{-3}\rangle_{3d}\,\{n(d_{xy}) + n(d_{x2-y2}) - n(d_{z2}) - \tfrac{1}{2}[n(d_{xz}) + n(d_{yz})]\} + (4/5)\,(1-R)\,\langle r^{-3}\rangle_{4p}\,\{1/2[n(p_x) + n(p_y)] - n(p_z)\}$ (eq. 6)

$q_{lat} = (1-\gamma_\infty) \sum_{i=1}^{n} \left(q_i/r_i^3\right) (3\cos^2\theta_i - 1)$ (eq. 7)

In general, for the low-spin pseudo-octahedral complexes, the valence contribution is close to zero and thus, many of such complexes have zero or small quadrupole splitting. This is not the case for $Pc(2-)Fe^{II}L_2$, $Pc(2-)Fe^{II}L'L''$, and $[Pc(2-)Fe^{II}X_2]^{2-}$ complexes. Our DFT calculations on the axially coordinated iron(II) phthalocyanines using a large array of the exchange-correlation functionals shown that:[26] (i) modern "pure" (0% Hartree-Fock exchange) functionals can accurately predict both isomer shifts and quadrupole splittings in a large number of iron(II) phthalocyanines; (ii) the axial ligands effectively modulate only the population of the iron d_{z2} orbital, while the population in the other iron-centered 3d orbitals remains nearly the same. Indeed, clear correlations were observed between the DFT-predicted NBO population in d_{z2} orbital and experimental quadrupole splittings (Figure 8).[26] These correlations are remarkable taking into consideration complexity of the valence and lattice contributions by the axial ligands. Another interesting observation is that the DFT-predicted and experimentally observed quadrupole splittings for $Pc(2-)Fe^{II}L_2$ complexes with organic amines (which can be described to a large extent as pure σ-donors) have a linear relationship with the Fe-N(ax) bond distances (Figure 8).

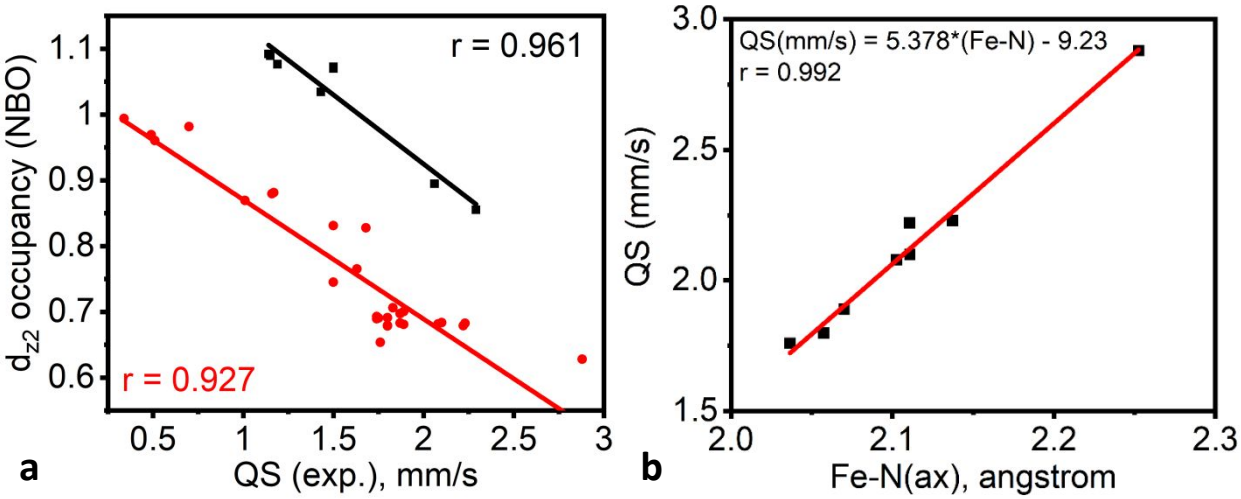

Figure 8. Correlation between NBO-predicted dz2 orbital population and the experimental quadrupole splitting in Pc(2-)$Fe^{II}L_2$ complexes (a); correlation between DFT-predicted quadrupole splitting and Fe-N(ax) bond distance in Pc(2-)$Fe^{II}L_2$ complexes with aliphatic amines (b).[26] Adapted with permission from *Inorg. Chem.* **2021**, *60*, 3690-3706. Copyright 2021 American Chemical Society.

The elongation of the Fe-N(ax) bond distance, in turn, reduces the singlet (ground state) and triplet energy gaps in $PcFeL_2$ complexes. Indeed, the DFT-predicted singlet-triplet energy gap for Pc(2-)$Fe^{II}(DABCO)_2$ complex (Figure 1) is very small (0.23 eV), which makes this complex an attractive candidate for the spin crossover system.[27] Although the low thermal stability of Pc(2-)$Fe^{II}(DABCO)_2$ complex precluded us from seeing such a transition, more stable compounds might achieve this goal. The low singlet-triplet energy gap also inspired us to study excited states dynamics of Pc(2-)$Fe^{II}(DABCO)_2$ complex. Again, a very small energy gap resulted in ultrafast (~200 fs) deactivation of the first excited state.

Conclusions and outlook

Despite a long history, iron phthalocyanines continue to inspire research curiosity, which translates in a number of applications. Our recent findings allow to generalize trends in spectroscopy and redox properties of the axially coordinated iron(II) phthalocyanines. Understanding of these trends allows a rational design of the systems with specifically localized redox centers, valence tautomerism, compounds that are able of singlet-triplet spin transitions, and singlet-triplet fission. Thus, although old and putatively trivial, these cheap and highly stable complexes have exciting potentials for future high-tech applications.

Authors contributions

CJZ and VNN wrote the manuscript.

Conflict of interest

There are no conflicts to declare.

Acknowledgements

Generous support from the NSF (CHE-2153081), Minnesota Supercomputing Institute, and the University of Tennessee to VN is greatly appreciated.

References

1. Gregory, P. *J. Porphyrins Phthalocyanines* **2000**, *4*, 432−437.

2. Erk, P.; Hengelsberg, H. In: *Porphyrin Handbook*, Kadish K. M, Smith K. M., Guilard R. (Eds.), Elsevier Science: San Diego, CA, **2003**; *Vol. 19*, 105−149.

3. Woehrle, D.; Schnurpfeil, G.; Makarov, S. G.; Kazarin, A.; Suvorova, O. N. *Makrogeterotsikly* **2012**, *5*, 191−202.

4. de la Torre, G.; Vazquez, P.; Agullo-Lopez, F.; Torres, T. *J. Mater. Chem.* **1998**, *8*, 1671−1683.

5. Sorokin, A. B. *Chem. Rev.* **2013**, *113*, 8152-8191.

6. V. N. Nemykin and E. A. Lukyanets, in: *Handbook of Porphyrin Science*, K. M. Kadish, K. M. Smith and R. Guilard (Eds.); World Scientific: Singapore, **2010**, *Vol 3*., pp 1 - 323.

7. Lever, A. B. P. *Inorg. Chem.* **1990**, *29*, 1271-1285.

8. Alexiou, C.; Lever, A. B. P. *Coord. Chem. Rev.* **2001**, *216-217*, 45-54.

9. Gouterman, M.; Wagniere, G.; Snyder, L. C. *J. Mol. Spectr.* **1963**, *11*, 108-127.

10. Nemykin, V. N.; Nevonen, D. E.; Osterloh, W. R.; Ferch, L. S.; Harrison, L. A.; Marx, B. S.; Kadish, K. M. *Inorg. Chem.* **2021**, *60*, 16626-16644.

11. Nemykin, V. N.; Purchel, A. A.; Spaeth, A. D.; Barybin, M. V. *Inorg. Chem.* **2013**, *52*, 11004-11012.

12. Dale, B. W. *Trans. Faraday Soc.* **1969**, *65*, 331-339.

13. Ough, E. A.; Stillman, M. J. *Inorg. Chem.* **1994**, *33*, 573-583.

14. Nemykin, V. N.; Polshina, A. E.; Chernii, V. Y.; Polshin, E. V.; Kobayashi, N. *Dalton Trans.* **2000**, 1019-1025.

15. Sumimoto, M.; Kawashima, Y.; Hori, K.; Fujimoto, H. *Dalton Trans.* **2009***,* 5737-5746.

16. Nevonen, D. E.; Ferch, L. S.; Schrage, B. R.; Nemykin, V. N. *Inorg. Chem.* **2022**, *61*, 8250-8266.

17. Schrage, B. R.; Zhou, W.; Harrison, L. A.; Nevonen, D. E.; Thompson, J. R.; Prosser, K. E.; Walsby, C. J.; Ziegler, C. J.; Leznoff, D. B.; Nemykin, V. N. *Inorg. Chem.* **2022**, *61*, 20177-20199.

18. Clack, D.W.; Yandle, J. R. *Inorg. Chem.* **1972**, *11*, 1738-1742.

19. Taube, R. *Pure Appl. Chem.* **1974**, *38*, 427-438.

20. Lever, A. B. P.; Wilshire, J. P. *Inorg. Chem.* **1978**, *17*, 1145-1151.

21. Tasso, T. T.; Furuyama, T.; Kobayashi, N. *Inorg. Chem.* **2013**, *52*, 9206-9215.

22. Kovarev, D. V.; Kuzmin, A. V.; Simonov, S. V.; Khasanov, S. S.; Otsuka, A.; Yamochi, H.; Saito, G.; Lyubovskaya, R. N. *Dalton Trans.* **2012**, 13841-13847.

23. Kaczmarzyk, T.; Jackowski, T.; Dzilinski, K. *Nucleonika* **2007**, *52*, S99-S103.

24. Nemykin, V. N.; Kobayashi, N.; Chernii, V. Y.; Belsky, V. K. *Eur. J. Inorg. Chem.* **2001**, 733-743.

25. Nevonen, D. E.; Ferch, L. S.; Chernii, V. Y.; Herbert, D. E.; van Lierop, J.; Nemykin, V. N.

J. Porphyrins Phthalocyanines **2020**, *24*, 894-903.

26. Nemykin, V. N.; Nevonen, D. E.; Ferch, L. S.; Shepit, M.; Herbert, D. E.; van Lierop, J. *Inorg. Chem.* **2021**, *60*, 3690-3706.

27. Nevonen, D. E.; Schaffner, J.; Hanrahan, P.; Shepit, M.; van Lierop, J.; Blank, D. A.; Nemykin, V. N. *J. Porphyrins Phthalocyanines* **2023**, *in press*,

28. Nemykin, V. N.; Hadt, R. G. *Inorg. Chem.* **2006**, *45*, 8297-8307.